发 光 学 报
CHINESE JOURNAL OF LUMINESCENCE

**Article ID**: 1000-7032(XXXX)XX-0001-10

# Synthesis, Photophysical and Chiroptical Properties of Pinene-based Chiral Iridium(III) Complexes

ZHOU Xuhao, LU Wenguang, ZHANG Ye, ZHENG Yu*

(*National Key Laboratory for the Development and Utilization of Forest Food Resources, Jiangsu Co-Innovation Center of Efficient Processing and Utilization of Forest Resources, Nanjing Forestry University, Nanjing* 210037, *China.*)

* *Corresponding Author, E-mail: zhengy@njfu. edu. cn*

**Abstract**: By introducing a chiral ligand induction strategy, two pairs of iridium complexes, Λ/Δ-Ir(pppy)$_2$(acac) and Λ/Δ-Ir(pppy)$_2$(tmd) (pppy = 2-phenyl-5,6-pinenopyridine), were synthesized and readily separated by conventional column chromatography. All complexes exhibit similar photophysical properties in solution. Remarkably, self-quenching is significantly suppressed even at high concentrations owing to the bulky pinene spacer that minimizes bimolecular interactions. Importantly, the Λ- and Δ- diastereomers exhibit intense and opposite CD and CPL signals with luminescence dissymmetry factors $g_{lum}$ on the order of $10^{-3}$. These results demonstrate that introducing a chiral, sterically hindered pinene moiety at the 5,6-positions of 2-phenylpyridine not only facilitates diastereomer separation but also effectively enables strong chiroptical responses while maintaining excellent anti-quenching properties.

**Keywords**: Iridium complexes; chiral synthesis; photophysical properties; chiroptical properties; pinene-derived ligand

**CLC number**: O482. 31 **Document code**: A

**DOI**: 10. 37188/CJL. 20260139 **CSTR**: 32170. 14. CJL. 20260139

# 蒎烯基手性铱配合物的合成、光物理与手性光学性质研究

周旭豪, 卢文广, 张烨, 郑煜*

(南京林业大学 森林食物资源挖掘与利用全国重点实验室,江苏省林业资源高效加工利用协同创新中心 江苏 南京 210037)

**摘要**: 通过引入手性配体诱导策略,利用常规柱层析方法分离得到了两对手性铱配合物 Λ/Δ-Ir(pppy)$_2$(acac)和 Λ/Δ-Ir(pppy)$_2$(tmd)(其中 pppy = 2-苯基-5,6-蒎烯并吡啶)。所有配合物在溶液中均表现出相似的光物理性质。值得注意的是,即使在高浓度下,由于体积庞大的蒎烯间隔基最大限度地减少了双分子相互作用,自猝灭现象也被显著抑制。重要的是,Λ-和 Δ-非对映异构体显示出强烈且相反的圆二色(CD)和圆偏振发光(CPL)信号,其发光不对称因子 $g_{lum}$ 达到 $10^{-3}$ 数量级。这些结果表明,在苯基吡啶的5,6-位引入手性且具有空间位阻的蒎烯基团,不仅有利于非对映异构体的分离,还能在保持优异抗猝灭性能的同时,有效实现强的手性光学响应。

**关 键 词**: 铱配合物; 手性合成; 光物理性质; 手性光学性质; 蒎烯基配体

## 1 Introduction

Over the past few years, cyclometalated iridium complexes have attracted considerable research interest for their applications in photoredox catalysis, [1-2] biosensing, [3-4] bioimaging, [5] and others. [6-8]

**收稿日期**: 2020-01-03; **修订日期**: 2020-01-05
**基金项目**: 国家自然科学基金(22201133)资助
Supported by National Natural Science Foundation of China (22201133)

Thanks to the spin-orbit coupling (SOC) of the heavy iridium ion, iridium complexes possess many outstanding photophysical properties, including high emission quantum yield, short phosphorescence lifetimes, large Stokes shifts, and high radiative decay rates. [9] These advantages enable them to be promising emitters that are used in organic light-emitting diodes (OLEDs). [10-13] Furthermore, chiral iridium complexes can act as luminescent materials to emit circularly polarized luminescence (CPL) that has potential applications in various fields, including optical data storage,[14] information encryption,[15] three-dimensional display,[16] microscopy probes,[17] and so on. [18-19] As a result, many strategies have been developed to synthesize chiral iridium complexes, such as resolution with chiral high-performance liquid chromatography (HPLC),[20-24] the utilization of a chiral ligand followed by separation of the resulting diastereomers,[25-30] and co-crystallization with an appropriate chiral counterion. [31] On the other hand, subtle modifications to the ligands of iridium complexes enable facile color tuning, while also modulating their photophysical and electroluminescent properties. [32-39] For example, in 2001, Lee and co-workers reported a green phosphorescence iridium complex Ir(pppy)$_3$, wherein a chiral pinene moiety was introduced into 2-phenylpyridine at 4,5-positions. [40] This modification significantly inhibited self-quenching in solution even at very high concentrations, owing to the pinene acts as a sterically hindered spacer. Moreover, this complex exhibited good electroluminescence performances even doped at high concentrations (up to 26%) with little concentration quenching. However, its chiroptical properties were not investigated. Employing the same chiral ligand, Zheng and coworkers synthesized a pair of iridium complexes (R/S)Ir(pppy)$_2$(acac). [41] They found that the self-quenching was efficiently inhibited due to the sterically hindered pinene substituents, which reduced the interaction between molecules. Importantly, using this iridium as emitter, the OLEDs showed a maximum luminance of 135 676 cd m$^{-2}$, a maximum current efficiency of 103 cd A$^{-1}$, and an EQE$_{max}$ of 28.0% with low efficiency roll-off. Unfortunately, these complexes showed very weak CPL signals, presumably due to they lack metal-centered chirality and the asymmetric carbons of ligand are far from the metal center.

In this work, we introduce a chiral and sterically hindered pinene moiety at the 5,6-positions of 2-phenylpyridine to further increase the steric hindrance, with the aim of enhancing the ability to inhibit self-quenching. In addition, the introduction of a chiral ligand would potentially facilitate the resolution of chiral iridium complexes. As a result, two pairs of iridium complexes, Λ/Δ-Ir(pppy)$_2$(acac) and Λ/Δ-Ir(pppy)$_2$(tmd), were synthesized using enantiopure 2-phenyl-5, 6-pinenopyridine as the main ligand and Hacac (or Htmd) as the auxiliary ligand. The corresponding Λ- and Δ- diastereomers were readily separated by conventional column chromatography. All the complexes exhibit similar photophysical properties in solution. It is observed that the self-quenching is significantly suppressed even at high concentrations, owing to the bulky pinene spacer that minimizes bimolecular interactions. Meanwhile, the diastereomers with Λ and Δ configurations at the metal center show intense circular dichroism (CD) and CPL signals with positive and negative Cotton effects, respectively, and $g_{lum}$ on the order of $10^{-3}$.

## 2 Experiment

### 2.1 Materials and Measurements

All solvents and materials were used as received from commercial suppliers without further purification. Flash column chromatography was performed using silica gel 60 (200-300 mesh). High-resolution mass spectrometry (HRMS) was recorded on a Q-TOF (AB SCIEX X500R with ESI source, and Agilent 7250 with EI source), which combines quadrupole precursor ion selection and a high-resolution accurate-mass (HR/AM) time of flight mass analyzer to deliver mass accuracy. All $^1$H NMR and $^{13}$C{$^1$H} NMR spectra were recorded on Bruker DRX600 and AMX-400 instruments. UV-vis absorption spectra were measured in dichloromethane solutions in 1 cm quartz cuvettes sealed with a screw cap and septum, using a Shimadzu UV-2600i UV-Vis

spectrophotometer. Steady-state emission spectra and phosphorescence lifetimes were measured using a Horiba FluoroMax-4 spectrofluorometer with appropriate long-pass filters to exclude stray excitation light from detection. Photoluminescence quantum yields of solution samples were determined relative to a standard of *fac*-Ir(ppy)$_3$ in dichloromethane, which has a reported fluorescence quantum yield ($\Phi$) of 0.4. Voltammetric experiments were performed using a DH7000D electrochemical workstation. The CD spectra were measured on a MOS-500 spectropolarimeter. The CPL spectra were measured on a Jasco CPL-300 spectrophotometer.

## 2.2 Synthesis of Chiral Iridium (III) complexes

Fig. 1 outlines the synthetic routes of two pairs of chiral Ir(III) complexes, which were synthesized using the literature methods.[42] Firstly, the reaction of enantiopure 2-phenyl-5, 6-pinenopyridine ligand with $IrCl_3 \cdot xH_2O$ in a 3:1 ethoxyethanol-$H_2O$ mixture at 125 °C mainly led to the formation of the corresponding dimers in homochiral fashion. Its worthy mention that these two diastereomers can be separated on silica gel chromatography, which is more synthetically convenient than the conventional chiral iridium complexes that typically rely on expensive and complicated chiral HPLC resolutions. Then, the individual diastereomer reacted with Hacac or Htmd in the presence of sodium carbonate ($Na_2CO_3$) in dichloromethane under reflux conditions, affording the final chiral iridium complexes.

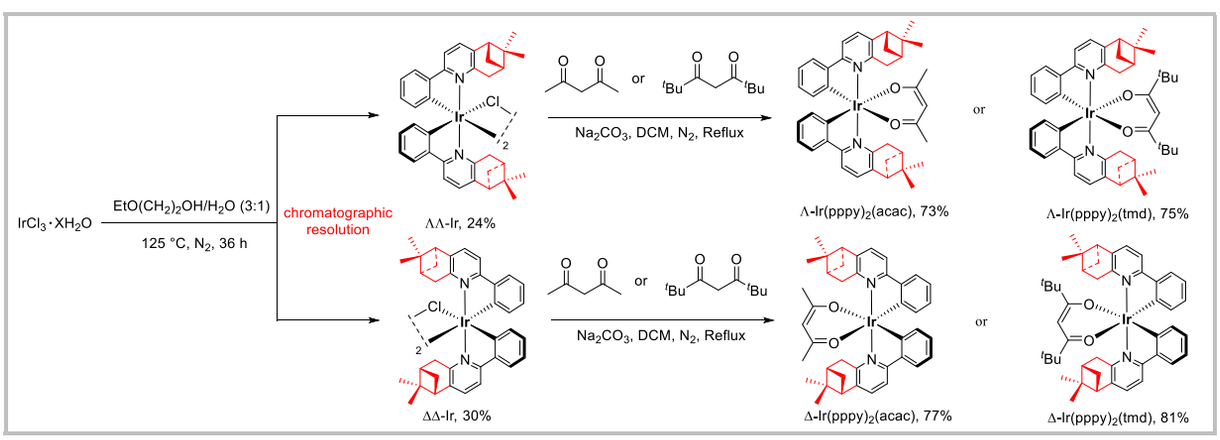


Fig.1 The synthetic route of four chiral Ir(III) complexes.

Λ-Ir(pppy)$_2$(acac): Yield: 73%. $^1$H NMR (600 MHz, $CDCl_3$) $\delta$ 7.57 (d, $J$ = 8.0 Hz, 2H), 7.49 (d, $J$ = 6.5 Hz, 2H), 7.27 (d, $J$ = 7.9 Hz, 2H), 6.82 – 6.77 (m, 2H), 6.65 – 6.60 (m, 2H), 6.36 (d, $J$ = 7.5 Hz, 2H), 5.23 (s, 1H), 3.34 (dd, $J$ = 18.7, 2.8 Hz, 2H), 3.21 (dd, $J$ = 18.7, 3.4 Hz, 2H), 2.81 (t, $J$ = 5.8 Hz, 2H), 2.63 (dt, $J$ = 10.3, 5.6 Hz, 2H), 2.20 (dt, $J$ = 6.1, 3.0 Hz, 2H), 1.58 (s, 6H), 1.39 (s, 6H), 1.29 (d, $J$ = 4.6 Hz, 2H), 0.70 (s, 6H). $^{13}$C{$^1$H} NMR (150MHz, $CDCl_3$) $\delta$ 185.4, 166.7, 160.8, 146.8, 144.4, 140.5, 134.6, 134.1, 127.8, 123.1, 120.9, 114.5, 101.3, 47.1, 40.3, 38.9, 35.6, 31.4, 28.2, 25.8, 21.0. HRMS-ESI *m/z*: [M+H]$^+$ Calculated for $C_{41}H_{44}IrN_2O_2$ 789.3027; Found 789.3037. CD (DCM): λ, nm ($\Delta\varepsilon$, $M^{-1}cm^{-1}$): 268 (38.8), 288 (28.6), 333 (23.4).

Δ-Ir(pppy)$_2$(acac): Yield: 77%. $^1$H NMR (600 MHz, $CDCl_3$) $\delta$ 7.58 (d, $J$ = 8.0 Hz, 2H), 7.51 (d, $J$ = 7.7 Hz, 2H), 7.28 (d, $J$ = 7.9 Hz, 2H), 6.81 (t, $J$ = 7.6 Hz, 2H), 6.61 (t, J = 7.3 Hz, 2H), 6.42 (d, $J$ = 7.7 Hz, 2H), 5.21 (s, 1H), 3.31 (dd, $J$ = 18.7, 3.2 Hz, 2H), 3.11 (dd, $J$ = 18.8, 2.9 Hz, 2H), 2.80 (d, $J$ = 5.8 Hz, 2H), 2.66 (dt, $J$ = 10.7, 5.7 Hz, 2H), 2.22 (dt, J = 6.1, 3.1 Hz, 2H), 1.59 (s, 6H), 1.38 (s, 6H), 1.24 (d, $J$ = 9.4 Hz, 2H), 0.79 (s, 6H). $^{13}$C{$^1$H} NMR (150 MHz, $CDCl_3$) $\delta$ 185.4, 166.6, 160.7, 146.8, 144.6, 140.2, 135.0, 134.7, 127.5, 123.1, 121.0, 114.6, 101.0, 47.0, 40.7, 38.7, 36.1, 31.7, 28.2, 25.9, 21.6. HRMS-ESI *m/z*: [M+H]$^+$ Calculated for $C_{41}H_{44}IrN_2O_2$ 789.3027; Found 789.3027. CD (DCM): λ, nm ($\Delta\varepsilon$, $M^{-1}cm^{-1}$): 268 (-36.3), 286 (22.3), 333 (-25.9).

Λ-Ir(pppy)$_2$(tmd): Yield: 75%. $^1$H NMR (600 MHz, $CDCl_3$) $\delta$ 7.55 (d, $J$ = 7.9 Hz, 2H), 7.51 (d,

*J* = 7.6 Hz, 2H), 7.22 (d, J = 7.9 Hz, 2H), 6.81 (t, *J* = 7.3 Hz, 2H), 6.62 (t, *J* = 7.1 Hz, 2H), 6.43 (d, *J* = 7.6 Hz, 2H), 5.50 (s, 1H), 3.15 – 3.03 (m, 4H), 2.77 (t, *J* = 5.7 Hz, 2H), 2.58 (dt, *J* = 9.5, 5.6 Hz, 2H), 2.10 (tt, *J* = 6.1, 3.0 Hz, 2H), 1.34 (s, 6H), 1.23 (d, *J* = 9.4 Hz, 2H), 0.79 (s, 18H), 0.69 (s, 6H). $^{13}C\{^1H\}$ NMR (151 MHz, $CDCl_3$) $\delta$ 193.8, 166.9, 160.7, 147.1, 146.7, 139.8, 134.6, 134.3, 127.1, 122.7, 120.3, 114.2, 90.8, 47.0, 41.0, 40.0, 38.9, 36.1, 31.4, 28.0, 25.8, 21.8. HRMS-ESI *m/z*: $[M+H]^+$ Calculated for $C_{47}H_{56}IrN_2O_2$ 873.3966; Found 873.3956. CD (DCM): λ, nm ($\Delta\varepsilon$, $M^{-1}cm^{-1}$): 266 (56.4), 293 (42.6), 335 (31.8).

Δ -Ir(pppy)$_2$(tmd): Yield: 81%. $^1H$ NMR (600 MHz, $CDCl_3$) $\delta$ 7.55 (d, *J* = 7.9 Hz, 2H), 7.52 (d, *J* = 7.6 Hz, 2H), 7.23 (d, *J* = 7.9 Hz, 2H), 6.81 (t, *J* = 7.2 Hz, 2H), 6.61 (t, *J* = 7.0 Hz, 2H), 6.51 (d, *J* = 7.5 Hz, 2H), 5.46 (s, 1H), 3.21 (dd, *J* = 19.0, 3.1 Hz, 2H), 2.94 (dd, *J* = 18.9, 2.9 Hz, 2H), 2.75 (t, *J* = 5.7 Hz, 2H), 2.64 – 2.58 (m, 2H), 2.11 (dt, *J* = 6.1, 3.1 Hz, 2H), 1.35 (s, 6H), 1.18 (d, *J* = 9.3 Hz, 2H), 0.76 (s, 6H), 0.75 (s, 18H). $^{13}C\{^1H\}$ NMR (150 MHz, $CDCl_3$) $\delta$ 194.1, 166.7, 160.8, 147.0, 146.6, 139.8, 135.5, 134.3, 127.1, 122.7, 120.4, 114.2, 90.2, 47.0, 41.0, 40.5, 38.8, 36.0, 31.6, 27.9, 25.9, 21.6. HRMS-ESI *m/z*: $[M+H]^+$ Calculated for $C_{47}H_{56}IrN_2O_2$ 873.3966; Found 873.3961. CD (DCM): λ, nm ($\Delta\varepsilon$, $M^{-1}cm^{-1}$): 266 (56.4), 293 (42.6), 335 (31.8).

## 3 Results and Discussion

The high diastereomeric purity of these four complexes was confirmed by $^1H$-NMR, and the absolute configuration of Λ-Ir(pppy)$_2$(tmd) was confirmed by X-ray crystallography. All four complexes display high configurational stability without any significant isomerization or decomposition upon leaving the complexes in the solid state in the fridge for two months. Their structures were characterized by nuclear magnetic resonance (NMR) spectroscopy and mass spectrometry. Single crystals of Λ -Ir(pppy)$_2$(tmd) suitable for testing were cultivated by allowing the solvent to slowly diffuse and evaporate. As shown in Fig. 2, Λ-Ir(pppy)$_2$(tmd) adopts a pseudo-octahedral coordination geometry, in which the Ir atom is surrounded by C and N atoms from two pppy ligands and two O atoms from Htmd. The bond lengths of Ir – C(14) and Ir – C(32) are 1.999(8) and 1.990(8) Å, while the bond lengths of Ir – N(1) and Ir – N(2) are 2.079(6) and 2.089(6) Å, respectively. Two Ir – O bonds are 2.169(5) and 2.155(5) Å, respectively. The angles of C(14) – Ir – N(1), C(14) – Ir – N(1), and O(1) – Ir – O(2) are 80.7(3)°, 81.1(3)° and 85.6(2)°, respectively. These bond data are close to those found in other cyclometalated Ir complexes. [24,41]

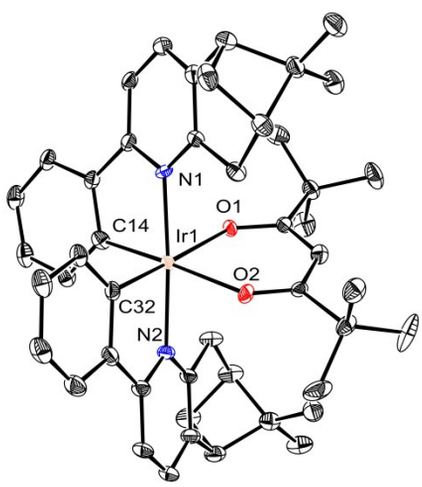


Fig.2 ORTEP diagram of Λ-Ir(pppy)$_2$(tmd) with the ellipsoids drawn at the 30 % probability level. Hydrogen atoms are omitted for clarity.

The normalized UV-visible absorption and photoluminescence (PL) spectra of the four diastereomerically pure Ir(III) complexes in dichloromethane at room temperature are illustrated in Fig. 3. All four complexes show almost identical spectra, indicating that metal-centered chirality and the auxiliary ligand have little influence on the steady-state photophysical properties. The strong bands around 272 nm should originate from π-π* transitions of the cyclometalated ligands. The weak bands at longer wavelength around 360-500 nm may be assigned to the mixture of the spin-allowed singlet metal-to-ligand charge transfer ($^1$MLCT) and triplet metal-to-ligand charge transfer ($^3$MLCT) transitions (Tab. 1). The phosphorescent properties of the four complexes were investigated using an excitation wavelength of 320 nm. They all exhibit green emissions with peaks around 509 nm and shoulders at around 530 nm. The lifetimes of Λ-Ir

$(pppy)_2(acac)$ and Λ-$Ir(pppy)_2(tmd)$ in degassed dichloromethane at different concentrations (from $1\times10^{-4}$ to $1\times10^{-6}$ mol/L) were then tested. The measured lifetimes were linearly correlated with each other, and could be fitted to the Stern-Volmer kinetics equation: $\tau_0/\tau = 1+k_q\tau_0[C]$. $\tau_0$ and $k_q$ were calculated to be 7.82 μs and $1.6\times10^8$ L/mol·$s^{-1}$ for Λ-$Ir(pppy)_2(acac)$ and 9.12 μs and $2.32\times10^8$ L/mol·$s^{-1}$ for Λ-$Ir(pppy)_2$(tmd), respectively. $k_q$ is below the diffusion-controlled limit of $10\times10^{10}$ L/mol·$s^{-1}$,[43] indicating that there exists weak concentration quenching in Λ-$Ir(pppy)_2(acac)$ and Λ-$Ir(pppy)_2(dpm)$ solution, which may be due to the high steric effect of the pinene moiety. The quantum efficiency of Λ/Δ-$Ir(pppy)_2(acac)$ and Λ/Δ-$Ir(pppy)_2$(tmd), measured in degassed dichloromethane solutions, was determined to be 9.8%, 8.3%, 11.7%, and 12.6%, respectively, with *fac*-$Ir(ppy)_3$ as reference (Tab. 1).

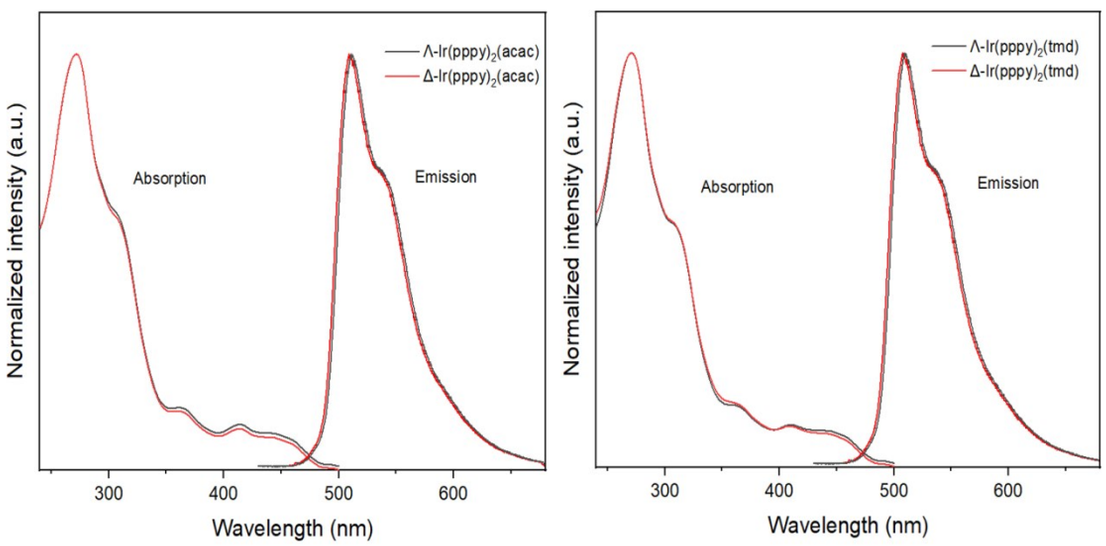


Fig.3 The UV-Vis and PL spectra of Λ/Δ-$Ir(pppy)_2(acac)$ and Λ/Δ-$Ir(pppy)_2$(tmd).

Tab. 1 The photophysical and electrochemical properties of complexes

| Complexes | Absorption/nm[a] | Emission/nm[b] | Φ (%)[c] | τ (μs)[d] | HOMO[e] | $E_g$/eV[f] | LUMO[g] |
|---|---|---|---|---|---|---|---|
| Λ-$Ir(pppy)_2(acac)$ | 271, 296, 363, 414, 450 | 511 (531) | 9.8 | 7.82 | −5.12 | 2.53 | −2.59 |
| Δ-$Ir(pppy)_2(acac)$ | 272, 304, 362, 414, 449 | 509 (529) | 8.3 | 6.51 | −5.16 | 2.53 | −2.63 |
| Λ-$Ir(pppy)_2$(tmd) | 272, 301, 365, 410, 444 | 509 (531) | 11.7 | 9.12 | −5.04 | 2.54 | −2.50 |
| Δ-$Ir(pppy)_2$(tmd) | 271, 298, 364, 409, 445 | 507 (530) | 12.6 | 8.47 | −5.11 | 2.54 | −2.57 |

[a]Measured in dichloromethane solution ($1.0\times10^{-5}$ M). [b]Measured in degassed dichloromethane ($1.0\times10^{-5}$ M), and shoulders in brackets. [c]In relative to *fac*-$Ir(ppy)_3$ in degassed dichloromethane solution. [d]Measured in degassed dichloromethane at 298 K with $\lambda_{ex}$ = 320 nm. [e]Measured from CV with ferrocene as the external reference, HOMO (eV) = $-(E^{ox}_{onset} + 4.8)$ eV. [f]Calculated from the onset of the absorption, $E_g = 1240/\lambda$. [g]LUMO (eV) = $E_g$ + HOMO.

The theoretical calculation was performed to gain a deeper understanding of the electronic structure of these two pairs of chiral complexes. The geometry optimizations and energy calculations were performed using density functional theory (DFT) at the B3LYP level with the 6-31G(d,p)/LanL2DZ basis set in Gaussian 16 in the gas phase. The frontier molecular orbitals of $Ir(pppy)_2(acac)$ and $Ir(pppy)_2$(tmd) were illustrated in Fig 4 (left). For the $Ir(pppy)_2$(acac), the HOMO is mainly distributed over the two phenyl rings of the pppy (45.30%) and the d orbitals of the iridium center (41.67%). In contrast, the LUMO is predominantly localized on the cyclometalated main ligands (92.30%). Both the HOMO and LUMO show negligible contributions from the ancillary ligand (acac), accounting for only 3.72% and 0.46%, respectively. The HOMO of $Ir(pppy)_2$(tmd) is similarly distributed over the two phenyl rings (45.83%) and the iridium d orbitals (40.82%), while the LUMO is mainly localized on the cyclometalated main ligands (90.09%). The contributions from the ancillary ligand remain minimal, at

3.83% for the HOMO and 1.75% for the LUMO, respectively. Overall, the frontier molecular orbital distributions of $Ir(pppy)_2(acac)$ and $Ir(pppy)_2(tmd)$ complexes are highly similar, indicating that substitution with the bulkier $^t$Bu group does not significantly alter the electronic structure of the metal-centered HOMO or the ligand-centered LUMO. However, the slightly increased LUMO contribution from the ancillary ligand in the $^t$Bu system (1.75% vs 0.46%) suggests a modest electronic perturbation, possibly arising from the stronger steric and inductive effects of the $^t$Bu substituent. The HOMO-LUMO energy gaps of these two compounds are -3.57 and -3.54 eV, respectively. Since the diastereomers have similar properties, Λ-$Ir(pppy)_2(acac)$ and Λ-$Ir(pppy)_2(tmd)$ were selected to study their electrochemical properties and energy levels of frontier molecular orbitals.

As shown in Fig. 4, Λ-$Ir(pppy)_2(acac)$ and Λ-$Ir(pppy)_2(tmd)$ have a chemically quasi-reversible oxidation in $CH_3CN$ solution, which can be attributed to the metal-centered Ir(III)/Ir(IV) oxidation couple. The onset oxidation potentials for Λ-$Ir(pppy)_2(acac)$ and Λ-$Ir(pppy)_2(tmd)$ were determined to be 0.32 and 0.25 V, respectively, with ferrocene as the external reference. Therefore, the HOMO energy levels of Λ/Δ-$Ir(pppy)_2(acac)$ and Λ/Δ-$Ir(pppy)_2(tmd)$ were calculated to be -5.12/-5.16 eV and -5.04/-5.11 eV, respectively, according to the empirical formula $E_{HOMO} = -(E^{ox}_{onset}+4.8)$eV. Their LUMO energy levels were obtained from $E_{LUMO} = E_{HOMO} + E_g$ ($E_g$, the optical bandgaps calculated from their absorption spectra using the formula $Eg = 1240/\lambda$ ) and calculated to be -2.59/-2.63 eV and -2.50/-2.57 eV, respectively.

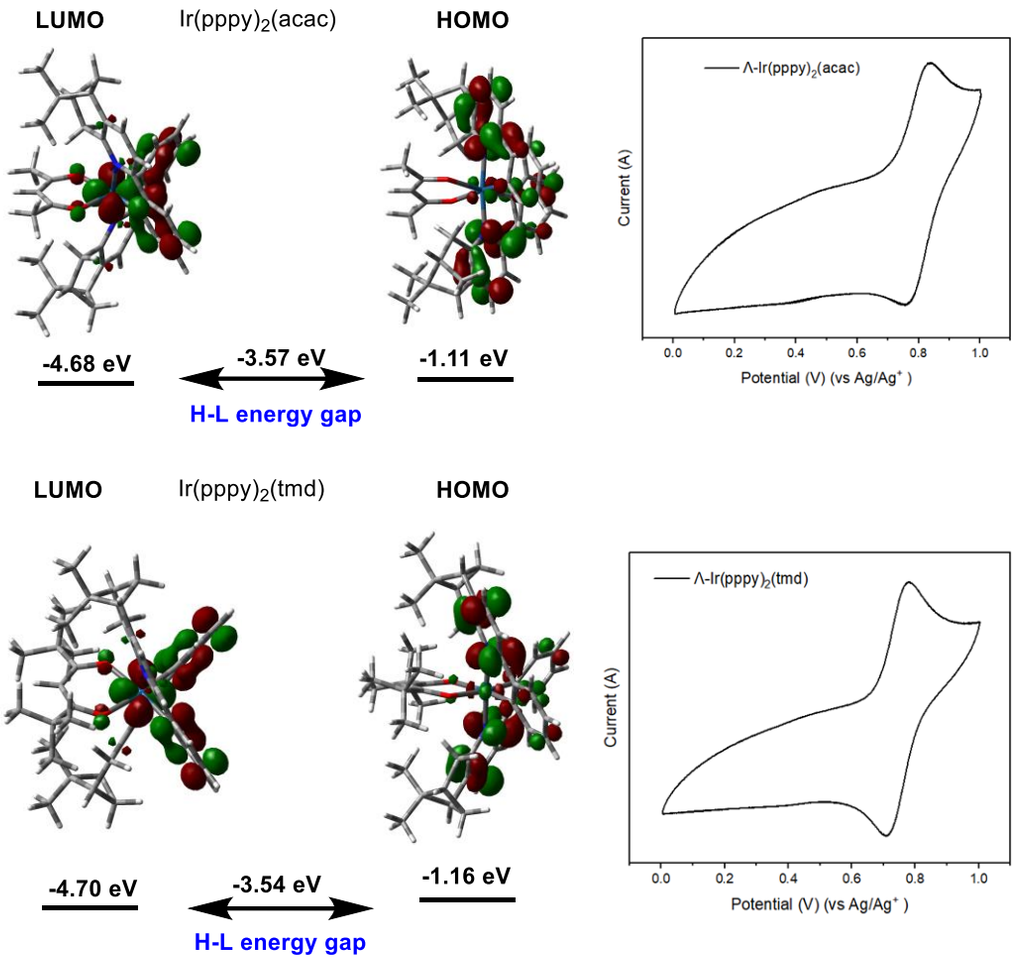


Fig.4 Frontier molecular orbitals and the cyclic voltammogram curves of $Ir(pppy)_2(acac)$ and $Ir(pppy)_2(tmd)$.

The experimental CD spectra of the four diastereomers were recorded in dichloromethane solution and are depicted in Fig. 5 (a, b). Each pair of diastereomers exhibits a near mirror-image relationship

with opposite polarization between 250-550 nm. For example, Λ-Ir(pppy)$_2$(acac) exhibits positive Cotton effects from 250 to 305 nm and 320 to 350 nm, and negative Cotton effects from 390 to 475 nm. In contrast, Δ-Ir(pppy)$_2$(acac) shows negative Cotton effects from 250 to 305 nm and 320 to 350 nm, and positive Cotton effects from 390 to 475 nm. Similar results are observed for Λ-Ir(pppy)$_2$(tmd) and Δ-Ir(pppy)$_2$(tmd), which exhibit mirror-image CD spectra with alternating negative and positive Cotton effects. The strong Cotton effects observed in the short-wavelength region are attributed to the absorption of an intramolecular π-system transition. In contrast, the weak Cotton effects appearing at the long-wavelength absorption band arise from MLCT. However, given that each pair of diastereomers bears identical chiral ligands, the overall CD activity in this spectral range is predominantly determined by the chiral configuration at the metal center. Finally, the circularly polarized luminescence was then examined for these four complexes at room temperature. The overall $g_{lum}$ values in solution are on the order of $10^{-3}$, which are similar to previously reported iridium complexes.[21-24] As shown in Fig. 5 (c), the two diastereomers Λ-Ir(pppy)$_2$(acac) and Δ-Ir(pppy)$_2$(acac) exhibit almost opposite CPL responses, with emission dissymmetry factors $g_{lum}$ of $-1.91 \times 10^{-3}$ (at 621 nm) and $1.52 \times 10^{-3}$ (at 586 nm), respectively. In addition, $g_{lum}$ values of Λ-Ir(pppy)$_2$(tmd) and Δ-Ir(pppy)$_2$(tmd) were determined to be $-1.55 \times 10^{-3}$ (at 589 nm) and $1.45 \times 10^{-3}$ (at 581 nm) respectively. The above characterizations reveal that the chiroptical properties of both the ground and excited states of the complexes are governed primarily by the configuration of the iridium center, while the asymmetric carbon center on the ligand appears to have little influence on the electronic and photophysical properties.

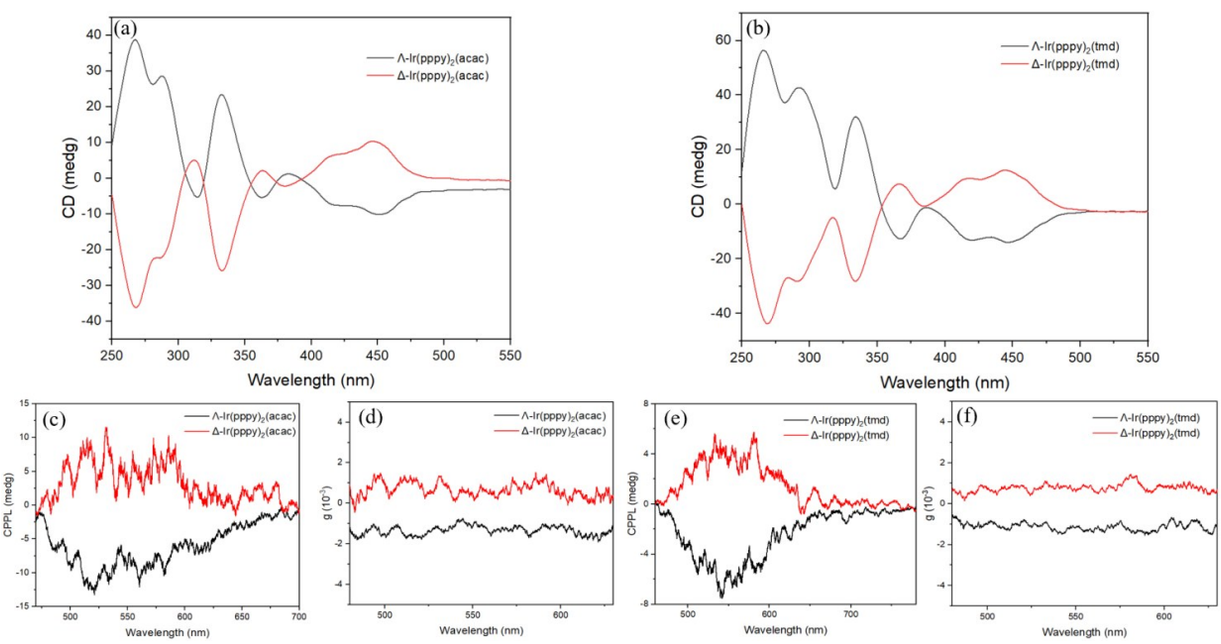


Fig.5 (a, b) CD spectra of Λ/Δ-Ir(pppy)$_2$(acac) and Λ/Δ-Ir(pppy)$_2$(tmd). (c, e) CPL spectra of Λ/Δ-Ir(pppy)$_2$(acac) and Λ/Δ-Ir(pppy)$_2$(tmd). (d, f) $g_{lum}$-wavelength curves of Λ/Δ-Ir(pppy)$_2$(acac) and Λ/Δ-Ir(pppy)$_2$(tmd).

## 4 Conclusion

In summary, we have designed and synthesized two pairs of chiral iridium complexes, Λ/Δ-Ir(pppy)$_2$(acac) and Λ/Δ-Ir(pppy)$_2$(tmd), by incorporating a sterically demanding ligand with the pinene unit fused at the 5, 6-positions of the 2-phenylpyridine ring. This structural modification serves two important purposes. First, the presence of the chiral pinene ligand allows straightforward separation of the Λ- and Δ-diastereomers using simple column chromatography, avoiding the need for chiral HPLC or chiral counterion crystallization. Second, the bulky pinene spacer efficiently suppresses self-quenching

in solution even at high concentrations. All complexes show similar absorption and emission properties, confirming that the photophysical behavior is largely governed by the cyclometalated iridium core. Notably, the Λ- and Δ-diastereomers display mirror-image CD and CPL signals with dissymmetry factors reaching $10^{-3}$, indicating that the chiral configuration at the metal center effectively dictates the chiroptical properties, while the remote lateral asymmetric carbon centers have virtually no influence.

Response Letter is available for this paper at: http://cjl. lightpublishing. cn/thesisDetails#10. 37188/CJL. 20220***(20220***为文章稿号).

**References:**


[1] ACKERMAN L G K, ALVARADO J I M, DOYLE A G. Direct C–C bond formation from alkanes using Ni-photoredox catalysis [J]. *J. Am. Chem. Soc.*, 2018, 140(43): 14059-14063.

[2] Li H Y, Fei M C, TROIANO J L, *et al*. Selective methane oxidation by heterogenized iridium catalysts [J]. *J. Am. Chem. Soc.*, 2023, 145(2): 769-773.

[3] HUANG T C, YU Q, LIU S J, *et al*. Phosphorescent iridium(III) complexes: a versatile tool for biosensing and photodynamic therapy [J]. *Dalton. Trans.*, 2018, 47(23): 7628-7633.

[4] Wu Y Y, SUTTON G D, HALAMIEEK M D S, *et al*. Cyclometalated iridium-coumarin ratiometric oxygen sensors: improved signal resolution and tunable dynamic ranges [J]. *Chem. Sci.*, 2022, 13(30): 8804–8812.

[5] TAN C P, ZHONG Y M, JI L N, *et al*. Phosphorescent metal complexes as theranostic anticancer agents: combining imaging and therapy in a single molecule [J], *Chem. Sci.*, 2021, 12(7): 2357–2367.

[6] FENG Z H, XIAN J H, CHEN F F, *et al*. Intermolecular interactions enhanced second harmony generation of iridium complex for bio-labeling [J]. *Chem. Eng. J.*, 2023, 458: 141503.

[7] WANG W H, LIU J H, NAO S C, *et al*. Affinity-based luminescent iridium(III) complexes for the detection of disease-related proteins [J]. *Inorganics.*, 2022, 10(11): 178.

[8] LEE L C C, LO K K W. Luminescent and photofunctional transition metal complexes: from molecular design to diagnostic and therapeutic application [J]. *J. Am. Chem. Soc.*, 2022, 144(32): 14420-14440.

[9] YERSIN H, RAUSCH A F, CZERWIENIEE R, *et al*. The triplet state of organo-transition metal compounds. Triplet harvesting and singlet harvesting for efficient OLEDs [J]. *Coord. Chem. Rev.*, 2011, 255(21-22): 2622-2652.

[10] YAN Z P, MAO M X, LIU Q M, *et al*. Rigidity-enhanced narrowband iridium(III) complexes with finely-optimized emission spectra for efficient pure-red electroluminescence [J]. *Adv. Funct. Mater.*, 2024, 34(38): 2402906.

[11] CHEN P, WU Q W, YANG G Y, *et al*. [3+2+1] iridium(III) complexes for high-efficiency saturated red organic light-emitting diodes [J], *Chem. Eng. J.*, 2025, 523: 168283.

[12] JIANG C G, TEETS T S. Impacts of ancillary ligand coordination modes on red-emitting cyclometalated iridium complexes [J]. *Inorg. Chem. Front.* 2024, 11(5): 1501-1510.

[13] LAI P N, BRYSACZ C H, ALAM M K, *et al*. Highly efficient red-emitting bis-cyclometalated iridium complexes [J]. *J. Am. Chem. Soc.*, 2018, 140(32): 10198-10207.

[14] HUCK N P M, JAGER W F, LANGE B D, *et al*. Dynamic control and amplification of molecular chirality by circular polarized light [J]. *Science.*, 1996, 273: 1686-1688.

[15] WANG X J, MA S, ZHAO B, *et al*. Frontiers in circularly polarized phosphorescent materials [J]. *Adv. Funct. Mater.*, 2023, 33(20): 2214364.

[16] LI X N, XIE Y J, LI Z. The Progress of Circularly Polarized Luminescence in Chiral Purely Organic Materials [J]. *Adv. Photonics Res.*, 2021, 2: 2000136.

[17] MACKENZIE L E, PALSSON L O, PARKER D, *et al*. Rapid time-resolved circular polarization luminescence (CPL) emission spectroscopy [J]. *Nat. Commun.*, 2020, 11(1): 1676

[18] NITTI A, PASINI D, Aggregation-induced circularly polarized luminescence: chiral organic materials for emerging optical technologies [J]. *Adv. Mater.*, 2020, 32(41): 1908021.

[19] ZHANG D W, LI M, CHEN C F. Recent advances in circularly polarized electroluminescence based on organic light-

emitting diodes [J]. *Chem. Soc. Rev.*, 2020, 49(5):1331-1343.

[20] LU G Z, WU Z G, WU R X, *et al.* Semitransparent circularly polarized phosphorescent organic light-emitting diodes with external quantum efficiency over 30% and dissymmetry factor close to $10^{-2}$ [J]. *Adv. Funct. Mater.*, 2021, 31(36): 2102898.

[21] LI T Y, ZHANG Y X, ZHOU Y H. Iridium(iii) phosphorescent complexes with dual stereogenic centers: single crystal, electronic circular dichroism evidence and circularly polarized luminescence properties [J]. *Dalton. Trans.*, 2016, 45(48):19234-19237.

[22] YAN Z P, LUO X F, LIAO K, *et al.* The Taiji and Eight Trigrams chemistry philosophy of chiral iridium(iii) complexes with triplex stereogenic centers [J]. *Dalton. Trans.*, 2018, 47(12):4045-4048.

[23] LI T Y, JING Y M, LIU X, *et al.* Circularly polarised phosphorescent photoluminescence and electroluminescence of iridium complexes [J]. *Sci. Rep.*, 2015, 5:14912.

[24] CHEN P, WU Q W, WANG F X, *et al.* Circularly polarized organic light-emitting diodes with chiral asymmetric [Ir($C_1$^$N_1$)($C_2$^$N_2$)(L^X)]-tris-heteroleptic iridium(iii) complexes [J]. *J. Mater. Chem. C.*, 2025, 13(42):21433

[25] HAN J M, GUO S, WANG J, *et al.* Circularly polarized phosphorescent electroluminescence from chiral cationic iridium (III) isocyanide complexes [J]. *Adv. Opt. Mater.*, 2017, 5(22):1700359

[26] HELLOU N, SREBRO-HOOPER M, FAVEREAU L, *et al.* Enantiopure cycloiridiated complexes bearing a pentahelicenic N-heterocyclic carbene and displaying long-lived circularly polarized phosphorescence [J]. *Angew. Chem. Int. Ed.*, 2017, 56(28):8236-8239.

[27] YAN Z P, LIAO K, HAN H B, *et al.* Chiral iridium(iii) complexes with four-membered Ir-S-P-S chelating rings for high-performance circularly polarized OLEDs [J]. *Chem. Commun.*, 2019, 55(57):8215-8218.

[28] BALLERINI L, GOURLAOUEN C, DELPORTE-PEBAY M, *et al.* Mono-$Ir^{III}$ versus heterobimetallic $Ir^{III}$-$Au^{I}$ complexes for circularly polarized luminescence [J]. *Chem. Eur. J.*, 2025, 31(44):e202501611

[29] ZHANG X Y, CHEN Z Q, LI D, *et al.* Highly efficient circularly polarized phosphorescent electroluminescence from iridium(iii) complexes with chiral ligands [J]. *J Mater. Chem. C.*, 2024, 12(11):3997-4004.

[30] KANBE A, YOKOI K, YAMADA Y, *et al.* Optical resolution of carboxylic acid derivatives of homoleptic cyclometalated iridium(III) complexes via diastereomers formed with chiral auxiliaries [J]. *Inorg. Chem.*, 2023, 62(29): 11325-11341.

[31] LI Z Q, WANG Y D, SHAO J Y, *et al.* Electrically amplified circularly polarized luminescence by a chiral anion strategy [J]. *Angew. Chem. Int. Ed.*, 2023, 62(20):e202302160.

[32] LI T Y, WU J, WU Z G, *et al.* Rational design of phosphorescent iridium(III) complexes for emission color tunability and their applications in OLEDs [J]. *Coord. Chem. Rev.*, 2018, 374:55-92.

[33] OU C J, QIU Y C, CAO C H, *et al.* Modulating the peripheral large steric hindrance of iridium complexes for achieving narrowband emission and pure red OLEDs with an EQE up to 32.0% [J]. *Inorg. Chem. Front.*, 2023, 10(3):1018-1026.

[34] WANG X Z, XU M X, WEN L L, *et al.* Modulating the excited-state properties of iridium(III) complexes for achieving narrowband deep-red/near-infrared electroluminescence [J]. *Inorg. Chem.*, 2025, 64(41):20714-20721.

[35] 吴少华,陆光照,钟祥永,等. 中性蓝光铱配合物及其OLED研究进展 [J]. 发光学报, 2024, 45(11):1794-1810.
WU S H, LU G Z, ZHONG X Y, *et al.* Research progress of neutral blue iridium complexes in OLEDs [J]. *Chin. J. Lumin.*, 2024, 45(11):1794-1810. (in Chinese)

[36] 陆光照,吴少华,于胜,等. 含四元环Ir-S-C-S骨架的高效红光铱(Ⅲ)配合物及其OLED性能 [J]. 发光学报, 2024, 45(9):1467-1477.
LU G Z, WU S H, YU S, *et al.* Efficient red iridium(III) complexes with four-membered ring Ir-S-C-S framework and OLED performance [J]. *Chin. J. Lumin.*, 2024, 45(9):1467-1477. (in Chinese)

[37] YAN Z P, ZHU X P, BI H, *et al.* Recent progress of narrowband iridium(iii) complexes for organic light-emitting diodes [J]. *Mater. Horiz.*, 2026, DOI: 10.1039/D6MH00003G.

[38] 常桥稳,陈祝安,王姿奥,等. 基于苯基喹啉配体修饰的铱磷光配合物及其高效纯红光有机电致发光器件 [J]. 发光学报, 2022, 43(10):1584-1588.
CHANG Q W, CHEN Z A, WANG Z A, *et al.* Iridium phosphorescent complexes based on modified phenylquinoline li-

gand and their high-efficiency pure red organic electroluminescent device [J]. *Chin. J. Lumin.*, 2022, 43(9): 1467-1477. (in Chinese)

[39] 陈俊,徐颖,徐超,等. 辅助配体功能化铱(Ⅲ)配合物近红外电致发光材料的合成及其性能[J]. 发光学报, 2022, 43(8): 1217-1226.
CHEN J, XU Y, XU C, *et al*. Synthesis and properties of near infrared-emitting iridium(Ⅲ) complexes with auxiliary ligand functionalized [J]. *Chin. J. Lumin.*, 2022, 43(8): 1217-1226. (in Chinese)

[40] XIE H Z, LIU M W, WANG O Y, *et al*. Reduction of self-quenching effect in organic electrophosphorescence emitting devices via the use of sterically hindered spacers in phosphorescence molecules [J]. *Adv. Mater.*, 2001, 13(16): 1245-1248.

[41] ZHOU Y H, XU Q L, HAN H B, *et al*. Highly efficient organic light-emitting diodes with low efficiency roll-off based on iridium complexes containing pinene sterically hindered spacer [J]. *Adv. Opt. Mater.*, 2016, 4(11): 1726-1731.

[42] ZHENG Y, HARMS K, ZHANG L L, *et al*. Enantioselective alkynylation of 2-trifluoroacetyl imidazoles catalyzed by bis-cyclometalated rhodium(III) complexes containing pinene-derived ligands [J]. *Chem. Eur J.*, 2016, 22(34): 11977-11981.

[43] MURTAZA Z, ZIPP A P, WORL L A, *et al*. Energy transfer in the "inverted region" [J]. *J. Am. Chem. Soc.*, 1991, 113(13): 5113-5114.

周旭豪(2002-),男,江西南昌人,硕士研究生,2024年于太原工业学院获得学士学位,主要从事有机光电材料和手性稀土材料与器件的研究。
E-mail: 2635602439@qq.com

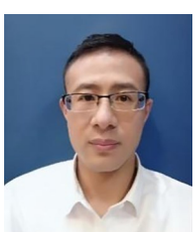

郑煜(1987-),男,安徽蚌埠人,博士,副教授,硕士生导师,2018年于德国马尔堡大学获得博士学位,主要从事有机光电材料和手性稀土材料与器件的研究。
E-mail: zhengy@njfu.edu.cn